

## Research Article

# Random Field Estimation with Delay-Constrained and Delay-Tolerant Wireless Sensor Networks

Javier Matamoros and Carles Antón-Haro

Centre Tecnològic de Telecomunicacions de Catalunya (CTTC), Parc Mediterrani de la Tecnologia,  
Av. Carl Friedrich Gauss 7, 08860-Castelldefels, Barcelona, Spain

Correspondence should be addressed to Javier Matamoros, javier.matamoros@cttc.es

Received 23 February 2010; Accepted 3 May 2010

Academic Editor: Davide Dardari

Copyright © 2010 J. Matamoros and C. Antón-Haro. This is an open access article distributed under the Creative Commons Attribution License, which permits unrestricted use, distribution, and reproduction in any medium, provided the original work is properly cited.

In this paper, we study the problem of random field estimation with wireless sensor networks. We consider two encoding strategies, namely, Compress-and-Estimate (C&E) and Quantize-and-Estimate (Q&E), which operate with and without side information at the decoder, respectively. We focus our attention on two scenarios of interest: *delay-constrained* networks, in which the observations collected in a particular timeslot must be immediately encoded and conveyed to the Fusion Center (FC); *delay-tolerant* (DT) networks, where the time horizon is enlarged to a number of consecutive timeslots. For both scenarios and encoding strategies, we extensively analyze the distortion in the reconstructed random field. In DT scenarios, we find closed-form expressions of the optimal number of samples to be encoded in each timeslot (Q&E and C&E cases). Besides, we identify buffer stability conditions and a number of interesting distortion versus buffer occupancy tradeoffs. Latency issues in the reconstruction of the random field are addressed, as well. Computer simulation and numerical results are given in terms of distortion versus number of sensor nodes or SNR, latency versus network size, or buffer occupancy.

## 1. Introduction

In recent years, research Wireless Sensor Networks (WSNs) has attracted considerable attention. This is in part motivated by the large number of applications in which WSNs are called to play a pivotal role, such as parameter estimation (i.e., moisture, temperature), event detection (leakage of pollutants, earthquakes, fires), or localization and tracking (e.g., border control, inventory tracking), to name a few [1].

Typically, a WSN consists of one Fusion Center (FC) and a potentially large number of sensor nodes capable of collecting and transmitting data to the FC over wireless links. In many cases, the underlying phenomenon being monitored can be modeled as a spatial random field. In these circumstances, the set of sensor observations are correlated, with such correlation being typically a function of their spatial locations (see, e.g., [2]). By effectively handling correlation in the data encoding process, substantial energy savings can be achieved.

In a *source coding* context, the work in [3] constitutes a generalization to sensor trees of Wyner-Ziv's pioneering studies [4]. The authors propose two coding strategies, namely Quantize-and-Estimate (Q&E) and Compress-and-Estimate (C&E), and analyze their performance for various networks topologies. The Q&E encoding scheme is a particularization of Wyner-Ziv's to scenarios with no side information at the decoder. Consequently, each sensor observation is encoded (and decoded) *independently*. Conversely, C&E turns out to be a *successive* Wyner-Ziv-based coding scheme and, for this reason, it is capable of exploiting spatial correlation.

In a context of random field *estimation* with WSNs, the pioneering work of [5] introduced the so-called "bit-conservation principle". The authors prove that, for spatially *bandlimited* processes, the bit budget per Nyquist-period can be arbitrarily reallocated along the quantization precision and/or the space (by adding more sensor nodes) axes, while retaining the same decay profile of the reconstruction

error. In [6] and, again, for bandlimited processes with *arbitrary* statistical distributions, the authors propose a mathematical framework to study the impact of the random sampling effect (arising from the adoption of contention-based multiple-access schemes) on the resulting estimation accuracy. For *Gaussian* observations, [7] presents a feedback-assisted Bayesian framework for adaptive quantization at the sensor nodes.

From a different perspective but still in a context of random field estimation, [2] proposes a novel MAC protocol which minimizes the attempts to transmit correlated data. By doing so, not only energy but also bandwidth is preserved. Besides, in [8], the authors investigate the impact of *random* sampling, as opposed to deterministic sampling (i.e., equally-spaced sensors) which is difficult to achieve in practice, in the reconstruction of the field. The main conclusion is that, whereas deterministic sampling pays off in the high-SNR regime, both schemes exhibit comparable performances in the low-SNR regime.

*Contribution.* In this paper, we address the problem of (nonnecessarily bandlimited) random field estimation with wireless sensor networks. To that aim, we adopt the Q&E and C&E encoding schemes of [3] and analyze their performance in two scenarios of interest: *delay-constrained* (DC) and *delay-tolerant* (DT) sensor networks. In DC scenarios, the observations collected in a particular timeslot must be immediately encoded and conveyed to the FC. In DT networks, on the contrary, the time horizon is enlarged to  $L$  consecutive timeslots. Clearly, this entails the use of local buffers but, in exchange, the distortion in the reconstructed random field is lower. To capitalize on this, we derive closed-form expressions of the distortion attainable in DT scenarios (unlike in [2, 6, 8], we explicitly take into account quantization effects). From this, we determine the optimal number of samples to be encoded in each of the  $L$  timeslots as a function of the channel conditions of that particular timeslot. This constitutes the first original contribution of the paper. Along with that, we identify under which circumstances buffers are stable (i.e., buffer occupancy does not grow without bound) and, besides, we study a number of distortion versus buffer occupancy tradeoffs. To the best of our knowledge, such analysis has not been conducted before in a context of random field estimation. Complementarily, we analyze the latency in the reconstruction of  $n$  consecutive realizations (i.e., those collected in one timeslot) of the random field, this being an original contribution, as well.

The paper is organized as follows. First, in Section 2, we present the signal and communication models, and provide a general framework for distortion analysis. Next, in Section 3, we focus on delay-constrained scenarios and particularize the aforementioned distortion analysis. In Sections 4 and 5 instead, we address delay-tolerant scenarios and analyze the behavior of the Q&E and C&E encoding schemes, respectively. Next, Section 6 investigates latency issues associated with DT networks. In Section 7, we present some computer simulations and numerical results and, finally, we close the paper by summarizing the main findings in Section 8.

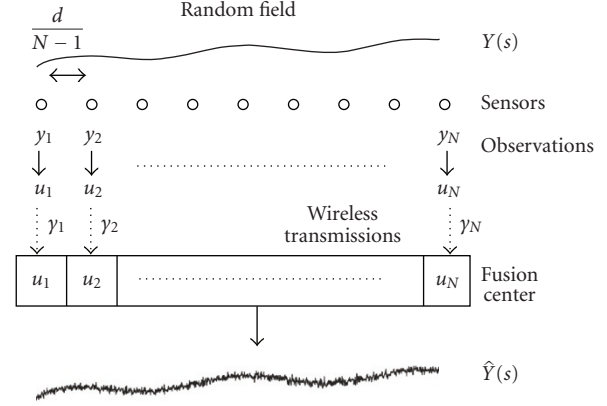


FIGURE 1: System model.

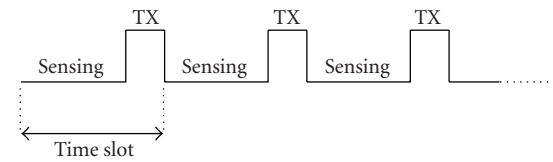


FIGURE 2: Sensing and transmission phases.

## 2. Signal Model

Let  $Y(s)$  be a one-dimensional random field defined in the range  $s \in [0, d]$ , with  $s$  denoting the spatial variable. As in [2, 8, 9], we adopt a stationary homogeneous Gaussian Markov Ornstein-Uhlenbeck (GMOU) model [10] to characterize the dynamics and spatial correlation of  $Y(s)$ . GMOU random fields obey the following linear stochastic differential equation

$$dY(s) = \theta Y(s)ds + \sigma W(s), \quad (1)$$

where, by definition,  $Y(s) \sim \mathcal{N}(0, \sigma_y^2)$  with  $\sigma_y^2 = \sigma/2\theta$ ,  $W(s)$  denotes Brownian Motion with unit variance parameter, and  $\theta, \sigma$  are constants reflecting the (spatial) variability of the field and its *noisy* behaviour, respectively. According to this model, the autocorrelation function is given by  $R_Y(s_1, s_2) = \sigma_y^2 e^{-\theta|s_2 - s_1|}$  and, hence, the process is not (spatially) bandlimited.

The random field is uniformly sampled by  $N$  sensor nodes, with intersensor distance given by  $d/(N-1) \simeq d/N$  (see Figure 1). The spatial samples can thus be readily expressed as follows [11]:

$$y_k = Y\left(k \frac{d}{N}\right) = e^{-\theta(d/2N)} y_{k-1} + n_k, \quad k = 1, \dots, N, \quad (2)$$

where  $n_k \sim \mathcal{N}(0, \sigma_y^2(1 - e^{-\theta(d/N)}))$ .

**2.1. Communication Model.** As shown in Figure 2, each time slot is composed of two distinctive phases namely, the *sensing* phase and the *transmission* phase. In the former, each sensor collects and stores in a local buffer a large block of  $n$  independent and consecutive observations

$\{y_k^{(i)}\}_{i=1}^n = \{y_k^{(1)}, \dots, y_k^{(n)}\}$ . Next, in the transmission phase,  $\{y_k^{(i)}\}_{i=1}^n$  is block-encoded into a length- $n$  codeword  $\{u_k^{(i)}(v_k)\}_{i=1}^n$  in codebook  $\mathcal{C}$  at a rate of  $R_k$  bits per sample. The encoding (quantization) process is modeled through the auxiliary random variable  $u_k = y_k + z_k$  with  $z_k$  standing for memoryless Gaussian noise with variance  $\sigma_{z_k}^2$  and statistically independent of  $y_k$  (for the ease of notation, we drop the sample index.) . The corresponding codeword index  $v_k \in \{1, \dots, 2^{nR_k}\}; k = 1 \dots N$  is then conveyed to the FC, in a total of  $m/N$  channel uses, over one of the *Northogonal* channels (for other encoding schemes, such as Compress-and-Estimate in Section 3.2,  $v_k$  denotes the index of the *bin* to which the codeword belongs to. For further details, see [3]). The codeword can only be reliably decoded at the FC if the encoding rate  $R_k$  satisfies

$$nR_k \leq \frac{m}{N} \log_2(1 + \text{SNR} \gamma_k) \text{ [b/s]}, \quad (3)$$

where SNR stands for the average signal-to-noise ratio experienced in the sensor-to-FC channels, and  $\gamma_1, \dots, \gamma_N$  denote the corresponding channel squared gains. In the sequel, such gains will be modeled as independent and exponentially-distributed unit-mean random variables (i.e., Rayleigh-fading channels) and independent over time slots (block fading assumption).

From the *set* of decoded codewords, the FC reconstructs the random field  $Y(s)$  for *all*  $s \in [0, d]$ . As a result of the spatial sampling process and the channel bandwidth constraint, the reconstructed field  $\hat{Y}(s)$  is subject to some distortion which, throughout this paper, will be characterized by the following metric

$$D(s) = \mathbb{E} \left[ \left| \hat{Y}(s) - Y(s) \right|^2 \right]; \quad \forall s \in [0, d]. \quad (4)$$

**2.2. Distortion Analysis: A General Framework.** For the distortion metric given by (4), the optimal estimator turns out to be the posterior mean given all the codewords  $\mathbf{u} = [u_1, \dots, u_N]^T$ ; that is, the MMSE estimator [12, Chapter 10]

$$\hat{Y}(s) = \mathbb{E}[Y(s) | \mathbf{u}]; \quad \forall s \in [0, d]. \quad (5)$$

For mathematical tractability, however, only the *two closest* decoded codewords, namely  $u_{k-1}$  and  $u_k$ , will be used to reconstruct  $Y(s)$  for *all* the corresponding intermediate spatial points (in noiseless scenarios, that is,  $\sigma_{z_k}^2 = 0$  for all  $k$ , this approach turns out to be optimal due to the Markovian property of GMOU processes. For the general case, yet suboptimal, it capitalizes on the codewords which retain more information on the random field at the spatial point  $s$ ) (see Figure 1), that is

$$\hat{Y}(s) = \mathbb{E}[Y(s) | u_{k-1}, u_k], \quad \forall s \in \left[ (k-1) \frac{d}{N}, k \frac{d}{N} \right]. \quad (6)$$

For the ease of notation and without loss of generality, in the sequel, we assume  $k = 1$  and, hence, the interval between

observations reads  $s \in [0, d/N]$ . From [12, Chapter 10], the distortion associated to the estimator (6) is given by

$$D_k(s) = \sigma_{Y(s)|u_{k-1}, u_k}^2 = \sigma_{Y(s)|u_{k-1}}^2 - \frac{\text{Cov}^2(Y(s), u_k | u_{k-1})}{\sigma_{u_k|u_{k-1}}^2}. \quad (7)$$

For our signal model and after some algebra, the various terms in the expression above can be computed as

$$\begin{aligned} \sigma_{Y(s)|u_{k-1}}^2 &= \left( \frac{1}{\sigma_y^2} + \frac{e^{-\theta s}}{(1 - e^{-\theta s})\sigma_y^2 + \sigma_{z_{k-1}}^2} \right)^{-1}, \\ \text{Cov}(Y(s), u_k | u_{k-1}) &= \mathbb{E}[(Y(s) - \mathbb{E}[Y(s) | u_{k-1}] | u_{k-1}) \\ &\quad \times (u_k - \mathbb{E}[u_k | u_{k-1}] | u_{k-1})] \\ &= \sqrt{e^{-\theta(d/N-s)}} \sigma_{Y(s)|u_{k-1}}^2, \\ \sigma_{u_k|u_{k-1}}^2 &= e^{-\theta(d/N-s)} \sigma_{Y(s)|u_{k-1}}^2 + (1 - e^{-\theta(d/N-s)})\sigma_y^2 + \sigma_{z_k}^2. \end{aligned} \quad (8)$$

It is worth noting that the variance of the quantization noise  $\sigma_{z_{k-1}}^2$  and  $\sigma_{z_k}^2$  are determined by the encoding strategy in use at the sensor nodes.

### 3. Delay-Constrained WSNs

In delay-constrained (DC) networks, the  $n$  samples collected in the sensing phase of a given timeslot must be necessarily encoded and transmitted to the FC in the corresponding transmission phase. Bearing this in mind, we particularize the analysis of Section 2.2 and compute the average distortion for the cases of Delay-Constrained Quantize-and-Estimate (QEDC) and Compress-and-Estimate (CEDC) encoding strategies.

**3.1. Quantize-and-Estimate: Average Distortion.** Here, each sensor encodes its observation regardless of any side information that could be made available to the FC. From [13], the following inequality holds for the rate at the output of the  $k$ th encoder (quantizer)

$$R_k \geq I(y_k; u_k) \text{ [b/sample]}, \quad (9)$$

with  $I(\cdot; \cdot)$  standing for the mutual information. As discussed before, the encoding (quantization) process is modeled through the auxiliary variable  $u_k = y_k + z_k$  with  $z_k \sim \mathcal{N}(0, \sigma_{z_k}^2)$  and statistically independent of  $y_k$  (see, e.g., [3, 14] for further details). The minimum rate per sample can be expressed as follows:

$$I(y_k; u_k) = H(u_k) - H(u_k | y_k) = \log \left( 1 + \frac{\sigma_y^2}{\sigma_{z_k}^2} \right) \text{ [b/sample]}. \quad (10)$$

From (3), (9), and (10) we have that, necessarily,

$$\frac{m}{N} \log_2(1 + \text{SNR} \cdot \gamma_k) \geq n \log_2 \left( 1 + \frac{\sigma_y^2}{\sigma_{z_k}^2} \right). \quad (11)$$

By taking equality in (11), the variance of the *quantization* noise yields

$$\sigma_{z_k}^2 = \frac{\sigma_y^2}{(1 + \text{SNR}\gamma_k)^{W/N} - 1}, \quad k = 1, \dots, N, \quad (12)$$

with  $W = m/n$  standing for the sample-to-channel uses ratio. By replacing (12) into (7), the distortion in an arbitrary spatial point  $s$  in the  $k$ th segment reads

$$\begin{aligned} D_k^{\text{QEDC}}(s) &= \left( \frac{1}{\sigma_{Y(s)|u_{k-1}}^2} + \frac{e^{-\theta(d/N-s)} \left( (1 + \text{SNR}\gamma_k(i))^{W/N} - 1 \right)}{\left( (1 + \text{SNR}\gamma_k(i))^{W/N} - 1 \right) (1 - e^{-\theta(d/N-s)}) \sigma_y^2 + \sigma_y^2} \right)^{-1}, \end{aligned} \quad (13)$$

with

$$\sigma_{Y(s)|u_{k-1}}^2 = \left( \frac{1}{\sigma_y^2} + \frac{e^{-\theta s} \left( (1 + \text{SNR}\gamma_k(i))^{W/N} - 1 \right)}{\left( (1 + \text{SNR}\gamma_k(i))^{W/N} - 1 \right) (1 - e^{-\theta s}) \sigma_y^2 + \sigma_y^2} \right)^{-1}. \quad (14)$$

The average distortion (over the spatial variable  $s$ ) in the  $k$ th network segment can be computed as

$$\bar{D}_k^{\text{QEDC}} = \frac{N}{d} \int_0^{d/N} D_k^{\text{QEDC}}(s) ds, \quad (15)$$

and, from this, the average distortion (over channel realizations) follows:

$$\bar{D}^{\text{QEDC}} = \mathbb{E}_{\gamma_1, \dots, \gamma_N} \left[ \frac{1}{N-1} \sum_{k=1}^{N-1} \bar{D}_{k+1}^{\text{QEDC}} \right]. \quad (16)$$

**3.2. Compress-and-Estimate: Average Distortion.** In Compress-and-Estimate encoding, the FC incorporates some side information into the decoding process. This extent can be exploited by the sensors in order to encode their observations more efficiently. For simplicity, we assume that only the codeword sent by the adjacent sensor,  $u_{k-1}$  will be used as side information for decoding codeword  $u_k$  (alternatively, we could use *all* the sensor observations but due to the spatial Markov property of the random field model, this is not expected to substantially decrease the encoding rate). Accordingly, the minimum rate per sample can be expressed as follows:

$$\begin{aligned} R_k &\geq I(\gamma_k; u_k | u_{k-1}) = H(u_k | u_{k-1}) - H(u_k | \gamma_k, u_{k-1}) \\ &= H(\gamma_k + z_k | u_{k-1}) - H(\gamma_k + z_k | \gamma_k) \\ &= \log_2 \left( 1 + \frac{\sigma_{\gamma_k | u_{k-1}}^2}{\sigma_{z_k}^2} \right) [\text{b/sample}], \end{aligned} \quad (17)$$

where the second equality is due to the fact that, again,  $u_k \leftrightarrow \gamma_k \leftrightarrow u_{k-1}$  form a Markov chain. Clearly, the codeword can be reliably transmitted if and only if

$$\frac{m}{N} \log_2(1 + \text{SNR} \cdot \gamma_k) \geq n \log_2 \left( 1 + \frac{\sigma_{\gamma_k | u_{k-1}}^2}{\sigma_{z_k}^2} \right). \quad (18)$$

By taking equality in (18), the minimum variance of the *quantization* noise  $\sigma_{z_k}^2$  follows:

$$\sigma_{z_k}^2 = \frac{\sigma_{\gamma_k | u_{k-1}}^2}{(1 + \text{SNR}\gamma_k)^{W/N} - 1}, \quad k = 1, \dots, N, \quad (19)$$

where  $\sigma_{\gamma_k | u_{k-1}}^2$  can be easily computed as:

$$\sigma_{\gamma_k | u_{k-1}}^2 = e^{-\theta(d/N-s)} \sigma_{Y(s)|u_k}^2 + \left( 1 - e^{-\theta(d/N-s)} \right) \sigma_y^2. \quad (20)$$

From (7), the distortion at an arbitrary spatial point  $s$  reads:

$$\begin{aligned} D_k^{\text{CEDC}}(s) &= \frac{\sigma_y^2 \sigma_{Y(s)|u_{k-1}}^2 \left( e^{\theta(d/N-s)} - 1 \right)}{\sigma_y^2 \left( e^{\theta(d/N-s)} - 1 \right) + \sigma_{Y(s)|u_{k-1}}^2} \\ &\quad + \frac{\sigma_{Y(s)|u_{k-1}}^4 \left( 1 + \text{SNR}\gamma_k \right)^{-W/N}}{\sigma_y^2 \left( e^{\theta(d/N-s)} - 1 \right) + \sigma_{Y(s)|u_{k-1}}^2}. \end{aligned} \quad (21)$$

with

$$\sigma_{Y(s)|u_{k-1}}^2 = \left( \frac{1}{\sigma_y^2} + \frac{e^{-\theta s} \left( (1 + \text{SNR}\gamma_k(i))^{W/N} - 1 \right)}{\left( (1 + \text{SNR}\gamma_k(i))^{W/N} - 1 \right) (1 - e^{-\theta s}) \sigma_y^2 + \sigma_{\gamma_{k-1} | u_{k-2}}^2} \right)^{-1}. \quad (22)$$

The average distortion for each network segment can be computed as follows:

$$\bar{D}_k^{\text{CEDC}} = \frac{N}{d} \int_0^{d/N} D_k^{\text{CEDC}}(s) ds \quad (23)$$

and, finally, the average distortion (over the channel realizations and network segments) yields:

$$\bar{D}^{\text{CEDC}} = \mathbb{E}_{\gamma_1, \dots, \gamma_N} \left[ \frac{1}{N-1} \sum_{k=1}^{N-1} \bar{D}_{k+1}^{\text{CEDC}} \right]. \quad (24)$$

## 4. Delay-Tolerant WSNs with Quantize-and-Estimate Encoding

Here, we impose a *long-term* delay constraint: the  $Ln$  samples collected in  $L$  consecutive timeslots must be conveyed to the FC in such  $L$  timeslots. In other words, sensors have now the flexibility to encode and transmit a *variable* number of samples in each time slot (according to channel conditions) and, by doing so, attain a lower distortion.

Let  $n_k(i) = \alpha_k(i)n$  be the number of samples encoded in  $m/N$  channel uses by sensor  $k$  in time-slot  $i$ . As in the previous section, we have that

$$\frac{m}{N} \log_2(1 + \text{SNR} \cdot \gamma_k(i)) \geq \alpha_k(i)n \log_2 \left( 1 + \frac{\sigma_y^2}{\sigma_{z_k}^2} \right); \quad (25)$$

$$k = 1, \dots, N.$$

By replacing  $\sigma_{z_k}^2$  from (25) into (7), the distortion per timeslot yields

$$D_{k,\alpha_k(i)}^{\text{QEDT}}(s) = \left( \frac{1}{\sigma_{Y(s)|u_{k-1}}^2} + \frac{e^{-\theta(d/N-s)} \left( (1 + \text{SNR}\gamma_k(i))^{W/N\alpha_k(i)} - 1 \right)}{\left( (1 + \text{SNR}\gamma_k(i))^{W/N\alpha_k(i)} - 1 \right) (1 - e^{-\theta(d/N-s)}) \sigma_y^2 + \sigma_y^2} \right)^{-1}. \quad (26)$$

In order to minimize the *average* distortion over the  $L$  timeslots at an arbitrary spatial point  $s$ , we need to solve the following optimization problem, implicitly, we are assuming that sensor  $(k-1)$ th encodes at a constant rate over timeslots. This extent will be verified later on in this section:

$$\begin{aligned} \min_{\alpha_k(1), \dots, \alpha_k(L)} \quad & \frac{1}{L} \sum_{i=1}^L \alpha_k(i) D_{k,\alpha_k(i)}^{\text{QEDT}}(s), \\ \text{s.t.} \quad & \sum_{i=1}^L \alpha_k(i)n = Ln, \end{aligned} \quad (27)$$

where the constraint in (27) is introduced to ensure the stability of the system. Unfortunately, a closed-form solution for  $\alpha_k(1), \dots, \alpha_k(L)$  cannot be obtained for this problem. Instead, we attempt to solve an approximate problem in which we assume that only codeword  $u_k$  will be used by the FC to reconstruct the random field  $Y(s)$  in  $s \in [(k-1)(d/N), k(d/N)]$ . Yet, suboptimal (the FC will actually use *both* codewords, namely  $u_k$  and  $u_{k-1}$ ), this solution outperforms those obtained in delay-constrained scenarios (see computer simulations section). Bearing all this in mind, the new cost function which follows from (26) can be readily expressed as

$$\begin{aligned} \check{D}_{k,\alpha_k(i)}^{\text{QEDT}}(s) &= \sigma_{Y(s)|u_k}^2 \\ &= \sigma_y^2 (1 - e^{-\theta s}) + \sigma_y^2 e^{-\theta s} (1 + \text{SNR}\gamma_k(i))^{-W/N\alpha_k(i)}. \end{aligned} \quad (28)$$

Clearly, only the second term in the summation of the cost function  $\check{D}_{k,\alpha_k(i)}^{\text{QEDT}}(s)$  is relevant to the optimization problem, which can be rewritten as

$$\begin{aligned} \min_{\alpha_k(1), \dots, \alpha_k(L)} \quad & \frac{1}{L} \sum_{i=1}^L \alpha_k(i) (1 + \text{SNR}\gamma_k(i))^{-W/N\alpha_k(i)} \\ \text{s.t.} \quad & \frac{1}{L} \sum_{i=1}^L \alpha_k(i) = 1. \end{aligned} \quad (29)$$

It is straightforward to show that this problem is convex. Hence, one can construct the Lagrangian as follows:

$$\begin{aligned} \mathcal{L}(\lambda, \alpha_k(1), \dots, \alpha_k(L)) &= \frac{1}{L} \sum_{i=1}^L \alpha_k(i) (1 + \text{SNR}\gamma_k(i))^{-W/N\alpha_k(i)} \\ &+ \lambda \left( \frac{1}{L} \sum_{i=1}^L \alpha_k(i) - 1 \right), \end{aligned} \quad (30)$$

where  $\lambda$  is the Lagrange multiplier. By setting the first derivative of (30) w.r.t.  $\alpha_k(i)$  to zero we obtain

$$\alpha_k^*(i) = \frac{W \ln(1 + \text{SNR}\gamma_k(i))}{N (1 - \omega_{-1}(\lambda^*/e))}, \quad (31)$$

with  $\omega_{-1}(\cdot)$  denoting the negative real branch of the Lambert function [15]. As for the computation of  $\lambda^*$ , the future channel gains  $(\gamma_k(i+1), \dots, \gamma_k(L))$  would be needed, in principle. However, as  $L \rightarrow \infty$  this noncasuality requirement vanishes: by the law of large numbers, we have that

$$\lim_{L \rightarrow \infty} \frac{1}{L} \sum_{i=1}^L \alpha_k^*(i) = \frac{W \mathbb{E}_y[\ln(1 + \text{SNR}y)]}{N (1 - \omega_{-1}(\lambda/e))} \quad (32)$$

and, hence,  $\lambda^*$  can be readily obtained by replacing this last expression into the constraint of (29), namely

$$\lambda^* = -\sigma_y^2 \left( \frac{W}{N} \bar{R} \ln(2) + 1 \right) e^{-(W/N)\bar{R} \ln(2)} \quad (33)$$

where we have defined

$$\bar{R} \triangleq \mathbb{E}_y[\log_2(1 + \text{SNR}y)]. \quad (34)$$

Finally, replacing  $\lambda^*$  into (31) yields

$$\alpha_k^*(i) = \frac{\log_2(1 + \text{SNR}\gamma_k(i))}{\bar{R}}; \quad i = 1, \dots, L, \quad k = 1, \dots, N, \quad (35)$$

and, by using  $\alpha_k^*(i)$  into (40), the quantization noise for the  $k$ th sensor node reads:

$$\sigma_z^2 = \sigma_{z_k}^2 = \frac{\sigma_y^2}{2^{(W/N)\bar{R}} - 1}; \quad i = 1, \dots, L, \quad k = 1, \dots, N. \quad (36)$$

which evidences that the encoding rate is constant over timeslots (as initially assumed) and over sensors too.

**4.1. Average Distortion in the Reconstructed Random Field.** By inserting  $\alpha_k^*(i)$  into the *original* cost function of (26), the distortion for an arbitrary point in the  $k$ th network segment reads

$$\begin{aligned} D_{k,\alpha_k(i)}^{\text{QEDT}}(s) &= D_k^{\text{QEDT}}(s) \\ &= \left( \frac{1}{\sigma_{Y(s)|u_{k-1}}^2} + \frac{e^{-\theta(d/N-s)} \left( 2^{(m/n)\bar{R}} - 1 \right)}{\left( 2^{(m/n)\bar{R}} - 1 \right) (1 - e^{-\theta(d/N-s)}) \sigma_y^2 + \sigma_y^2} \right)^{-1}. \end{aligned} \quad (37)$$

Interestingly, distortion is not a function of the channel gain experienced by the  $k$ th sensor in timeslot  $i$  (i.e., distortion does not depend on  $\alpha_k^*(i)$ ). As a result and unlike in QEDC encoding, the distortion experienced in every timeslot  $i = 1, \dots, L$  is identical. This can be useful in applications where a constant distortion level is needed.

After some tedious manipulations, the average distortion in the *entire* reconstructed random field can be expressed as

$$\begin{aligned} \bar{D}^{\text{QEDT}} &= \frac{1}{N-1} \sum_{k=1}^{N-1} \frac{N}{d} \int_0^{d/N} D_{k+1}^{\text{QEDT}}(s) ds \\ &= \frac{\left( (\sigma_y^2 + \sigma_z^2)^2 e^{\theta d/N} + \sigma_y^4 \right) \theta d/N}{\left( (\sigma_y^2 + \sigma_z^2)^2 e^{\theta d/N} - \sigma_y^4 \right) \theta d/N} \\ &\quad - \frac{2\sigma_y^4 (\sigma_y^2 + \sigma_z^2) (e^{\theta d/N} - 1)}{\left( (\sigma_y^2 + \sigma_z^2)^2 e^{\theta d/N} - \sigma_y^4 \right) \theta d/N} \end{aligned} \quad (38)$$

**4.2. Buffer Stability Considerations.** In order to derive a closed-form solution of the optimal number of samples to be encoded in each time slot ( $\alpha_k^*(i)$ ), in (32) we let the number of timeslots  $L$  grow to infinity. Clearly, this might lead to a situation where buffer occupancy grows without bound, that is, to buffer instability. To avoid that, we will encode and transmit a (slightly) higher number of samples per timeslot, namely

$$\alpha_k'(i)n = \frac{\log_2(1 + \text{SNR}\gamma_k(i))}{\bar{R} - \delta} n > \alpha_k^*(i)n, \quad (39)$$

with  $0 < \delta < \bar{R}$ . By doing so, one can prove (see the appendix) that buffers are stable. Unsurprisingly, this come at the expense of an increased distortion in the estimates (see computer simulation results in Section 7).

## 5. Delay-Tolerant WSNs with Compress-and-Estimate Encoding

As in previous section, we let  $n_k(i) = \alpha_k(i)n$  be the number of samples encoded in  $m/N$  channel uses (i.e., one timeslot). Again, the rate at the output of the C&E encoder must satisfy

$$\frac{m}{N} \log_2(1 + \text{SNR} \cdot \gamma_k(i)) \geq \alpha_k(i)n \log_2 \left( 1 + \frac{\sigma_{y_k|u_{k-1}}^2}{\sigma_{z_k}^2} \right). \quad (40)$$

To stress that expression (40) differs from (25) in that the C&E encoder assumes that the FC will use  $u_{k-1}$  to *decode*  $u_k$  and, hence,  $\sigma_{y_k}^2$  has been replaced by  $\sigma_{y_k|u_{k-1}}^2$ . Therefore, from

(7) and the definition of  $\sigma_{y_k|u_{k-1}}^2$  in (20), we have that for the current block of  $\alpha_k(i)n$  samples the distortion reads

$$\begin{aligned} D_{k,\alpha_k(i)}^{\text{CEDT}}(s) &= \frac{\sigma_y^2 \sigma_{Y(s)|u_{k-1}}^2 (e^{\theta(d/N-s)} - 1)}{\sigma_y^2 (e^{\theta(d/N-s)} - 1) + \sigma_{Y(s)|u_{k-1}}^2} \\ &\quad + \frac{\sigma_{Y(s)|u_{k-1}}^4 (1 + \text{SNR}\gamma_k(i))^{-m/\alpha_k(i)n}}{\sigma_y^2 (e^{\theta(d/N-s)} - 1) + \sigma_{Y(s)|u_{k-1}}^2}. \end{aligned} \quad (41)$$

By averaging over  $L$  timeslots, the following optimization problem results:

$$\begin{aligned} \min_{\alpha_k(1), \dots, \alpha_k(L)} \quad & \frac{1}{L} \sum_{i=1}^L \alpha_k(i) D_{k,\alpha_k(i)}^{\text{CEDT}}(s), \\ \text{s.t.} \quad & \sum_{i=1}^L \alpha_k(i)n = Ln. \end{aligned} \quad (42)$$

Solving this problem leads to a closed-form solution that is identical to that of the QEDT case, namely,

$$\alpha_k^*(i) = \frac{\log_2(1 + \text{SNR}\gamma_k(i))}{\bar{R}}. \quad (44)$$

Finally, replacing  $\alpha_k^*(i)$  into (40) yields

$$\sigma_{z_k}^2 = \frac{\sigma_{y_k|u_{k-1}}^2}{2^{(W/N)\bar{R}} - 1}; \quad i = 1, \dots, L, \quad k = 1, \dots, N, \quad (45)$$

that is, the encoding rate in CEDT networks is constant over sensors and timeslots, as implicitly assumed in the score function (43). To remark, the stability analysis of Section 4.2 also applies here.

**5.1. Average Distortion in the Reconstructed Random Field.** By inserting  $\alpha_k^*(i)$  into the original cost function of (43), the distortion for an arbitrary point in the  $k$ th segment reads

$$\begin{aligned} D_{k,\alpha_k(i)}^{\text{CEDT}}(s) &= \frac{\sigma_y^2 \sigma_{Y(s)|u_{k-1}}^2 (e^{\theta(d/N-s)} - 1)}{\sigma_y^2 (e^{\theta(d/N-s)} - 1) + \sigma_{Y(s)|u_{k-1}}^2} \\ &\quad + \frac{\sigma_{Y(s)|u_{k-1}}^4 2^{-(W/N)\bar{R}}}{\sigma_y^2 (e^{\theta(d/N-s)} - 1) + \sigma_{Y(s)|u_{k-1}}^2}. \end{aligned} \quad (46)$$

As in the QEDT case, distortion is not a function of the channel gain experienced by the  $k$ th sensor in timeslot  $i$ . Hence, the distortion experienced in every timeslot  $i = 1, \dots, L$  is identical. Therefore, the average distortion for

each network segment can be computed in a closed form as follows:

$$\begin{aligned} \bar{D}_k^{\text{CEDT}} &= \frac{N}{d} \int_0^{d/N} D_k^{\text{CEDT}}(s) \\ &= \frac{\left( (\sigma_y^2 + \sigma_{z_{k-1}}^2) (\sigma_y^2 + \sigma_{z_k}^2) e^{\theta d/N} + \sigma_y^4 \right) \theta d/N}{\left( (\sigma_y^2 + \sigma_{z_{k-1}}^2) (\sigma_y^2 + \sigma_{z_k}^2) e^{\theta d/N} - \sigma_y^4 \right) \theta d/N} \\ &\quad - \frac{\sigma_y^4 (2\sigma_y^2 + \sigma_{z_{k-1}}^2 + \sigma_{z_k}^2) (e^{\theta d/N} - 1)}{\left( (\sigma_y^2 + \sigma_{z_{k-1}}^2) (\sigma_y^2 + \sigma_{z_k}^2) e^{\theta d/N} - \sigma_y^4 \right) \theta d/N}. \end{aligned} \quad (47)$$

Finally, the average distortion in the *whole* reconstructed random field yields

$$\bar{D}^{\text{CEDT}} = \frac{1}{N-1} \sum_{k=1}^{N-1} \bar{D}_{k+1}^{\text{CEDT}}. \quad (48)$$

## 6. Latency Analysis

In delay-tolerant networks, each sensor encodes and transmits a variable number of samples per timeslot. As a result, the time elapsed until the FC receives the first  $n$  samples from *all* the  $N$  sensors in the network (which allows for the reconstruction of the first  $n$  realizations of the random field) is unavoidably larger than in delay-constrained networks. In this section, we attempt to characterize such latency. To that aim, we start by analyzing the time needed for *one* sensor to transmit  $n$  consecutive samples of the random field. Next, we derive the latency of the QEDT and CEDT encoding strategies, respectively.

*6.1. Latency Analysis for a Single Sensor Node.* Let  $n_k^*(i) = \lfloor \alpha_k^*(i)n \rfloor$  be the number of samples encoded in  $m/N$  channel uses in timeslot  $i$ . The probability that  $l = 0, \dots, n-1$  samples are encoded in arbitrary timeslot  $i$  can be expressed as

$$p_l = \Pr(n_k^*(i) = l) \quad (49)$$

$$= \Pr\left(\frac{l}{n} \leq \alpha_k^*(i) < \frac{l+1}{n}\right); \quad l = 0, \dots, n-1. \quad (50)$$

Besides, we define

$$p_n = \Pr(n_k^*(i) \geq n) \quad (51)$$

$$= \Pr(\alpha_k^*(i) \geq 1). \quad (52)$$

On that basis, we model our system as an absorbing Markov chain [16, Chapter 8] with  $n$  *transient* states ( $\mathcal{S}_1, \dots, \mathcal{S}_{n-1}$ )

and one *absorbing* state ( $\mathcal{S}_n$ ) defined as follows (see, Figure 3):

$$\mathcal{S}_l = \begin{cases} l \text{ samples have been transmitted} \\ \text{in previous timeslots,} \\ l = 0, \dots, n-1, \\ n \text{ or more samples have been transmitted} \\ \text{in previous timeslots,} \\ l = n. \end{cases} \quad (53)$$

The transition matrix  $\mathbf{P}$  of an absorbing Markov chain has the following canonical form:

$$\mathbf{P} = \begin{bmatrix} \mathbf{Q} & \mathbf{r} \\ \mathbf{0}^T & 1 \end{bmatrix}, \quad (54)$$

where  $\mathbf{Q}$  denotes the  $(n+1) \times (n+1)$  transient matrix and  $\mathbf{r}$  is a  $(n+1) \times 1$  nonzero vector (otherwise the absorbing state could never be reached from the transient states). The entries of the matrix  $\mathbf{Q}$  can be computed as follows:

$$q_{l,j} = \begin{cases} 0 & j < l, \\ p_{j-l} & \text{otherwise.} \end{cases} \quad (55)$$

The entries of the  $(n+1) \times 1$   $\mathbf{r}$  vector, which denote the probability of absorption from each transient states, are given by

$$r_l = 1 - \sum_{j=0}^{n-1} q_{l,j}; \quad l = 0, \dots, n-1. \quad (56)$$

Our goal is to characterize the time elapsed until the absorbing state is reached or, in other words, the time needed to transmit  $n$  consecutive samples of the local observation of the random field at sensor  $k$  (i.e., sensor latency). For an absorbing Markov chain, the time to absorption,  $\tau$ , is a random variable which obeys the so-called Discrete Phase-type (DPH) distribution. From [17], the probability mass and cumulative distribution functions can be expressed as:

$$f_\tau(t) = \Pr(\tau = t) = \boldsymbol{\pi}^T \mathbf{Q}^{t-1} \mathbf{r}; \quad t = 1, \dots, \infty \quad (57)$$

$$F_\tau(t) = \Pr(\tau \leq t) = 1 - \boldsymbol{\pi}^T \mathbf{Q}^t \mathbf{1}; \quad t = 1, \dots, \infty \quad (58)$$

where the  $(n+1) \times 1$  vector  $\boldsymbol{\pi}$  is used to define the initial conditions. Since we assume that initially no samples have been transmitted, this yields

$$\boldsymbol{\pi}^T = [1, 0, \dots, 0]^T. \quad (59)$$

From all the above, the *average* time to absorption reads:

$$\mathbb{E}[\tau] = \sum_{t=1}^{\infty} t f_\tau(t). \quad (60)$$

Alternatively, from [16, Chapter 8], one can compute

$$\mathbf{u} = (\mathbf{I} - \mathbf{Q}_1)^{-1} \mathbf{1} \quad (61)$$

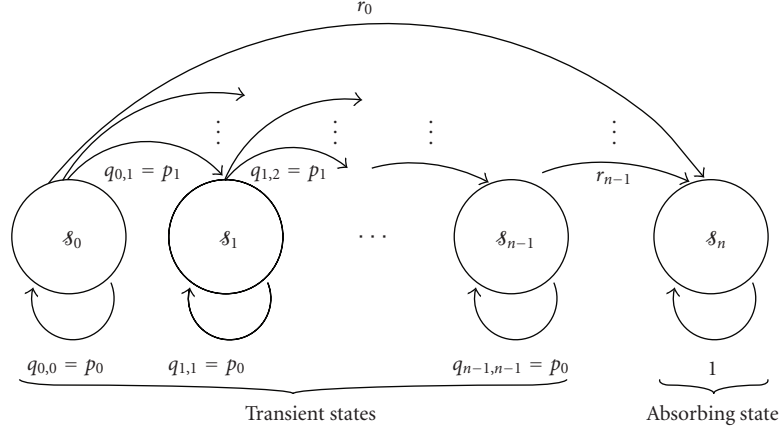


FIGURE 3: An absorbing Markov chain.

the elements of which account the average time to absorption from state  $s_0 \dots s_n$ . Consequently, the average sensor latency is given by its first element, namely,  $\mathbb{E}[\tau] = \mathbf{u}(1)$ .

Finally, we need to derive a closed-form expression for the set of probabilities  $\{p_0, p_1, \dots, p_n\}$  defined in (50) and (52). From (35), we have that

$$\alpha_k^*(i) = \frac{\log_2(1 + \text{SNR}\gamma_k(i))}{\bar{R}}. \quad (62)$$

with  $\bar{R} = \mathbb{E}_\gamma[\log_2(1 + \gamma\text{SNR})]$  and, hence,

$$\begin{aligned} p_l &= \Pr\left(\frac{l}{n} \leq \alpha_k^*(i) < \frac{l+1}{n}\right) \\ &= \Pr\left(\frac{l}{n}\bar{R} \leq \log_2(1 + \text{SNR}\gamma_k(i)) < \frac{l+1}{n}\bar{R}\right) \\ &= F_\gamma\left(\frac{2^{((l+1)/n)\bar{R}} - 1}{\text{SNR}}\right) - F_\gamma\left(\frac{2^{(l/n)\bar{R}} - 1}{\text{SNR}}\right) \end{aligned} \quad (63)$$

for  $l = 0, \dots, n-1$  and  $p_n = 1 - F_\gamma((2^{\bar{R}} - 1)/\text{SNR})$ . For Rayleigh-fading channels, the CDF of the channel gain is given by  $F_\gamma(x) = 1 - e^{-x}$ .

**6.2. Latency Analysis for QEDT Encoding.** At this point, the interest lies in characterizing the time elapsed until the  $N$  sensors in the network encode and transmit their first  $n$  samples of the random field. Let  $\Psi$  be a random variable which accounts for QEDT latency, namely

$$\Psi = \max_{k=1, \dots, N} \tau_k, \quad (64)$$

where  $\tau_k$  stands for the latency associated to the individual sensor  $k$  as defined in the previous section. Since, on the one hand, sensors experience i.i.d fading channels and, on the other, codewords from different sensors are decoded independently, then  $\tau_1, \dots, \tau_N$  turn out to be i.i.d. DPH random variables with marginal pmf's and CDFs given by

(57) and (58), respectively. From all the above, the CDF of the latency associated to QEDT encoding reads

$$\begin{aligned} F_\Psi(t) &= \Pr(\Psi \leq t) = \Pr\left(\max_k \tau_k \leq t\right) \\ &= \Pr(\tau_1 \leq t, \tau_2 \leq t, \dots, \tau_N \leq t) \\ &= F_\tau^N(t) = \left(1 - \boldsymbol{\pi}^T \mathbf{Q}^t \mathbf{1}\right)^N, \quad t = 1, \dots, \infty. \end{aligned} \quad (65)$$

The probability mass function can be computed as

$$\begin{aligned} f_\Psi(t) &= \Pr(\Psi = t) \\ &= F_\Psi(t) - F_\Psi(t-1) \\ &= \left(1 - \boldsymbol{\pi}^T \mathbf{Q}^t \mathbf{1}\right)^N - \left(1 - \boldsymbol{\pi}^T \mathbf{Q}^{t-1} \mathbf{1}\right)^N, \quad t = 1, \dots, \infty. \end{aligned} \quad (66)$$

and, from this last expression, the average latency yields

$$\mathbb{E}[\Psi] = \sum_{t=1}^{\infty} t f_\Psi(t). \quad (67)$$

Intuitively, latency is a monotonically increasing function in the number of sensors (the more sensors, the larger the time needed to collect all samples). This extent will be verified in Section 7 (Simulation and numerical results).

**6.3. Latency Analysis for CEDT Encoding.** The latency analysis for CEDT strategies is far more involved due to the successive encoding of data that C&E schemes entail. In general, this does not allow for the derivation of closed-form expressions and, thus, we will resort to an approximate (yet accurate) model.

In order for the FC to successfully decode the codeword received from sensor  $k$ , the codeword sent by the adjacent sensor  $k-1$  must have been decoded first. Consequently, the codeword sent by the  $N$ th sensor will be the last one to be decoded. Since sensors experience i.i.d. fading channels (and, thus, the number of observations received from different

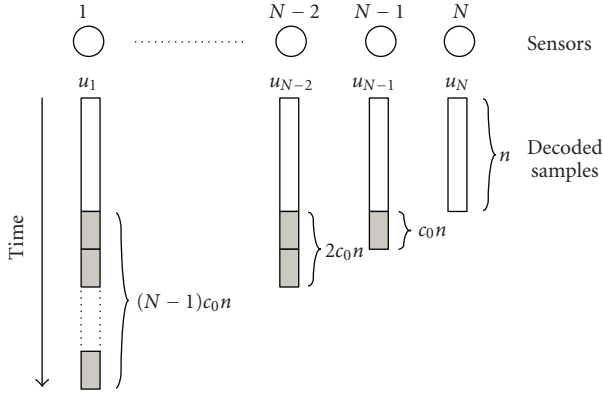


FIGURE 4: Approximate CEDT decoding for latency analysis.

sensors are not time-aligned), when the first  $n$  samples sent by sensor  $N$  are ready to be decoded, a total of  $n + c_0n > n$  samples from sensor  $N - 1$  have already been decoded on average. Accordingly, a total of  $n + (N - 1)c_0n$  samples from sensor #1 have already been decoded too (see Figure 4). Hence, the first  $n$  realizations of the *entire* random field can be reconstructed if, equivalently,  $n + (N - 1)c_0n$  samples sent by the first sensor have already been decoded by the FC. The encoding/decoding process for the first sensor is identical in C&E and Q&E schemes and, hence, in order to compute the latency for the reconstruction of the *random field*, it suffices to compute the time to absorption for an *individual* sensor (sensor #1) as we did in Section 6.1. The only change with respect to the model given in (54) is that the Markov chain has now a total of  $n + (N - 1)c_0n$  states (instead of  $n$ ) and, hence, the size and elements of matrix  $\mathbf{Q}$  and vectors  $\boldsymbol{\pi}$  and  $\mathbf{r}$  in (57) and (58) must be adjusted accordingly.

As for parameter  $c_0$ , which exclusively depends on the pdf of the sensor-to-FC channel gains, it can only be determined empirically (see next section).

## 7. Simulations and Numerical Results

Figure 5 depicts the (per timeslot) distortion in the reconstructed random field for both the QEDC and QEDT encoding strategies and different SNR values. For the QEDC strategy, we show the average value along with the  $\pm\sigma$  confidence interval (to recall that, unlike in the QEDT case, the distortion in QEDC encoding varies from timeslot to timeslot). Several conclusions can be drawn. First, for each curve there exists an optimal operating point; that is, a network size for which distortion can be minimized. The intuition behind this fact is that, despite that spatial variations of the random field are better captured by a denser grid of sensors, for a total bandwidth constraint the available rate per sensor progressively diminishes, this resulting into a more rough quantization of the observations. Thus, the optimal trade-off between these two effects needs to be identified. Second, the distortion associated to delay-tolerant strategies is, as expected, lower than for delay-constrained ones. Moreover, the lower the average SNR in the sensor-to-FC channels (namely, sensors with lower transmit power),

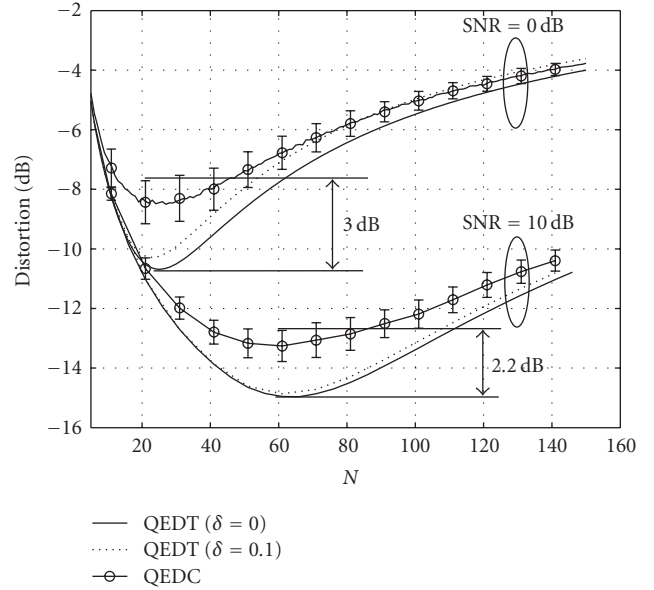
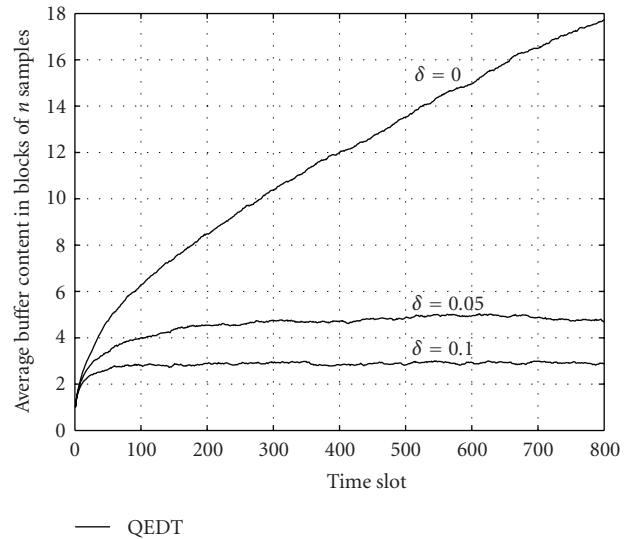
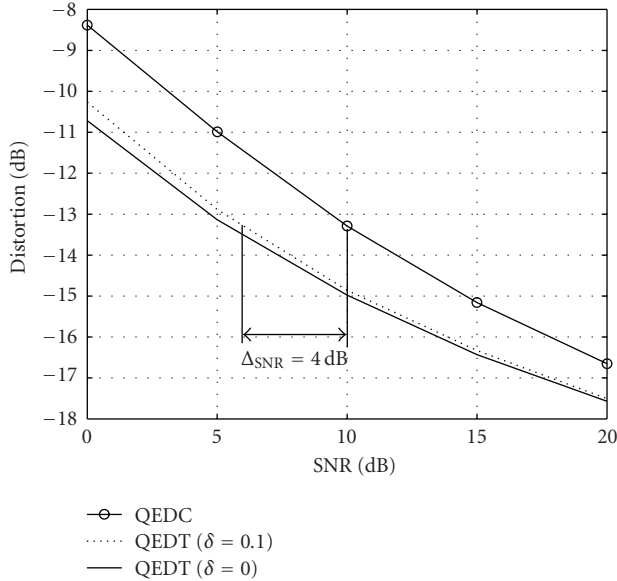
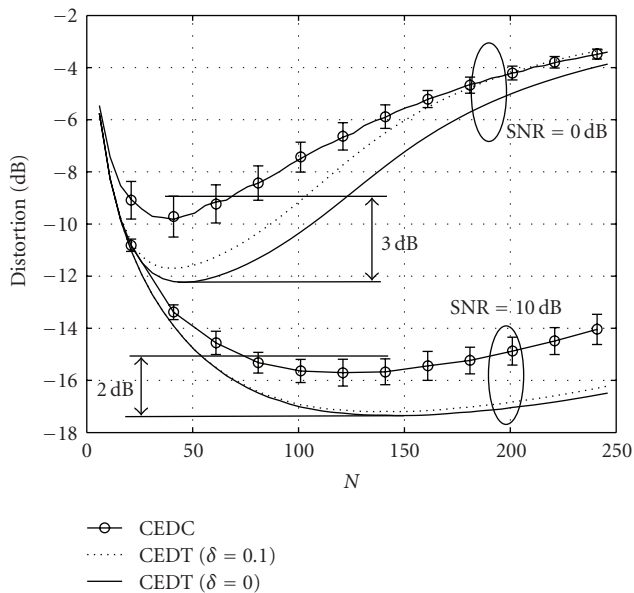

 FIGURE 5: Average distortion versus network size  $N$  ( $W = 150, \theta d = 10$ ).


FIGURE 6: Average buffer occupancy versus time (SNR = 0 dB).

the higher the gain (up to 3 dB for SNR = 0 dB). Third, guaranteeing buffer stability in the QEDT scheme only results into a marginal penalty in distortion, as shown in the curves labeled with  $\delta = 0$  and  $\delta = 0.1$ . Complementarily, in Figure 6, we depict buffer occupancy for several values of  $\delta$ . For  $\delta = 0$ , the system is clearly unstable. Conversely, by letting  $\delta$  take positive values, for example, for  $\delta = 0.1$  as in Figure 5, the average buffer occupancy can be kept under control (with a relatively small average buffer occupancy of  $3n$  samples, in this case). Clearly, increasing  $\delta$  has a two-fold effect: the average buffer occupancy diminishes but, simultaneously, the resulting distortion increases.

The rate at which distortion decreases for the QEDC and QEDT schemes (evaluated at their respective optimal

FIGURE 7: Average distortion versus SNR ( $W = 150, \theta_d = 10$ ).FIGURE 8: QEDT encoding: average distortion versus network size ( $W = 150, \theta_d = 10$ ).

operating points) for an increasing SNR is shown in Figure 7. For intermediate distortion values, the gap is approximately 4 dB. That is, for a prescribed distortion level, the energy consumption in delay-constrained networks is 2.5 times higher.

Figure 8 illustrates the average distortion in the reconstructed random field for the CEDC and CEDT encoding strategies. As in quantize-and-estimate encoding, there exists an optimal number of sensors nodes. Finding such  $N^*$  reveals particularly useful for random fields with low SNR per sensor, since the curve is sharper in this case. The gap between the minimum distortion attainable by the CEDC and CEDT schemes (which results from an

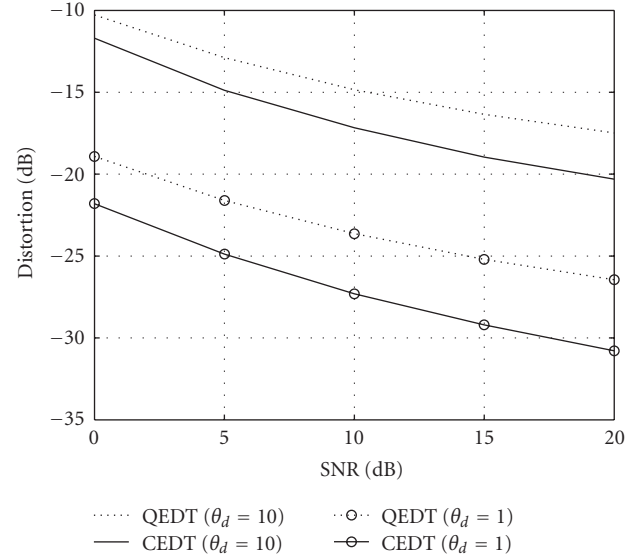
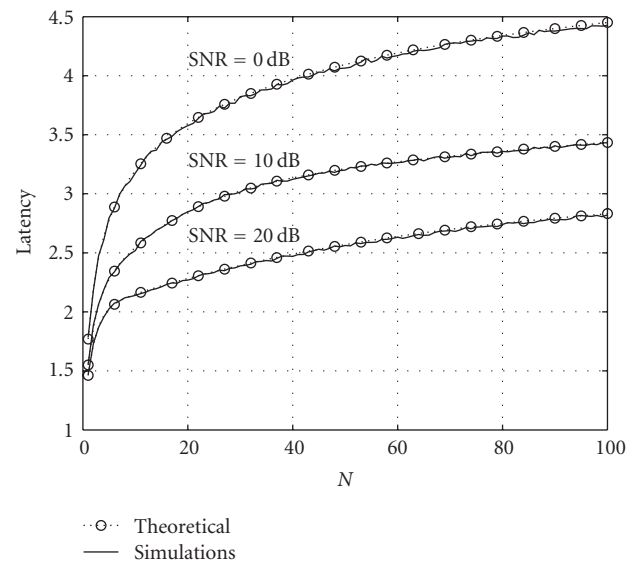
FIGURE 9: Distortion versus SNR ( $W = 150$ ).

FIGURE 10: CEDT encoding: average latency versus network size.

adequate exploitation of channel fluctuation in the delay-tolerant approach) is approximately 2-3 dB. Concerning buffer occupancy-distortion tradeoffs, the same comments as in the quantize-and-estimate case apply.

Next, in Figure 9, we compare the distortion attained by QEDT/CEDT encoding strategies for random fields with low and high spatial variabilities ( $\theta_d = 1, \theta_d = 10$ , resp.). Due to the fact that CEDT is capable of exploiting spatial correlation, it always outperforms QEDT. Moreover, the higher the spatial correlation ( $\theta_d = 1$ ), the larger the gap between the curves.

Finally, in Figures 10 and 11 we depict the average latency for the QEDT and CEDT strategies, respectively.

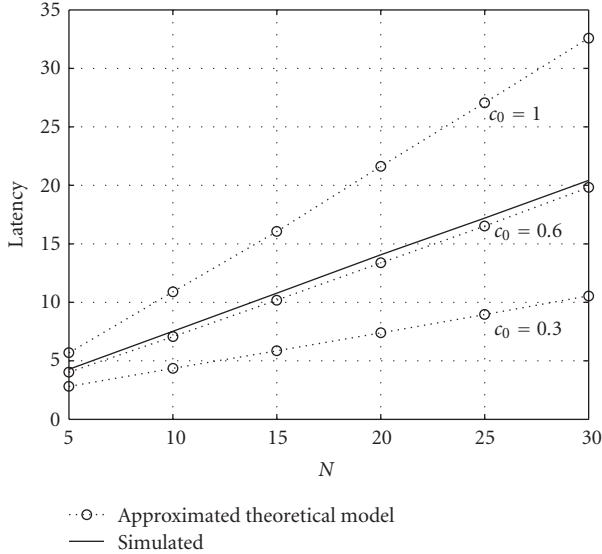


FIGURE 11: Average latency versus network size.

Interestingly, there exists a trade-off in terms of attainable distortion versus latency. Whereas in CEDT encoding latency exhibits a *linear* increase in the number of sensors, in QEDT encoding latency grows *logarithmically* (i.e., more slowly). However, CEDT schemes attain a lower distortion than QEDT ones. Besides, in Figure 10 it is also worth noting the perfect match between simulations and numerical results and, unsurprisingly, that the higher the average SNR, the lower the latency. Also, Figure 11 reveals that by using an appropriate value of  $c_o$  (i.e.,  $c_o = 0.6$ ), the latency associated to the approximate model described in Section 6.3 matches the actual one.

## 8. Conclusions

In this paper, we have extensively analyzed the problem of random field estimation with wireless sensor networks. In order to characterize the dynamics and spatial correlation of the random field, we have adopted a stationary homogeneous Gaussian Markov Ornstein-Uhlenbeck model. We have considered two scenarios of interest: delay-constrained (DC) and delay-tolerant (DT) networks. For each scenario, we have analyzed two encoding schemes, namely, quantize-and-estimate (QE) and compress-and-estimate (CE). In all cases (QEDC, QEDT, CEDC and CEDT), we have carried out an extensive analysis of the average distortion experienced in the reconstructed random field. Moreover, for the QEDT and CEDT strategies we have derived closed-form expressions of (i) the average distortion in the estimates, and (ii) the optimal number of samples of the random field to be encoded in each timeslot (under some simplifying assumptions). Interestingly, the resulting per-timeslot distortion in DT scenarios is deterministic and constant whereas, in DC scenarios, it ultimately depends on the fading conditions experienced in each timeslot. Next, we have focused on the latency associated to the QEDT and CEDT strategies. We

have modeled our system as an absorbing Markov chain and, on that basis, we have fully characterized the pdf, CDF, and the average latency for the QEDT case. For CEDT encoding, we have identified an approximate system model suitable for the computation of the average latency. Simulation results reveal that, under a total bandwidth constraint, there exists an optimal number of sensors for which the distortion in the reconstructed random field can be minimized (QEDC, QEDT, CEDC and CEDT cases). This constitutes the best trade-off in terms of, on the one hand, the ability to capture the spatial variations of the random field and, on the other, the persensor channel bandwidth available to encode observations. Besides, the distortion associated to delay-tolerant strategies is, as expected, lower than for delay-constrained ones: some 2-3 dB for both the QE and CE encoding schemes. Moreover, buffer occupancy can be kept at very moderate levels (3 timeslots) with a marginal penalty in terms of distortion (less than 0.3 dB). We also observe that CE schemes effectively exploit the spatial correlation and, by doing so, attain a lower distortion than their QE counterparts (DC and DT scenarios). As far as latency is concerned, we have empirically shown that CEDT exhibits a *linear* increase in the number of sensors whereas in QEDT encoding latency grows *logarithmically* (i.e., more slowly). However, CEDT schemes attain a lower distortion than QEDT ones. Besides, for the QEDT case, there is a perfect match between simulations and the theoretical model and, for the CEDT case, latency can be accurately represented by adequately parameterizing the aforementioned approximate system model.

## Appendix

### Buffer Stability Analysis

We want to prove that buffers are stable (i.e., their occupancy is bounded) for large  $L$ . Let  $b_k(i)$  denote the number of samples in the buffer of the  $k$ th sensor in time slot  $i$ , with initial conditions given by  $b_k(0) = L_0 n$ . After  $L$  timeslots, the increase in the number of samples stored in the buffer can be expressed as

$$b_k(L) - b_k(0) = Ln - \sum_{i=1}^L \alpha'_k(i)n, \quad (\text{A.1})$$

where  $Ln$  accounts for the number of samples generated in those  $L$  timeslots, and  $\sum_{i=1}^L \alpha'_k(i)n$  with

$$\alpha'_k(i) = \frac{\log_2(1 + \text{SNR}\gamma_k(i))}{\bar{R} - \delta} > \alpha_k^*(i), \quad (\text{A.2})$$

stands for the actual number of samples encoded and transmitted by the  $k$ th sensor node. The probability of experiencing an increase greater than  $\epsilon n$  in the number of samples stored reads

$$\begin{aligned} \Pr(b_k(L) - b_k(0) \geq \epsilon n) &= \Pr\left(Ln - \sum_{i=1}^L \alpha'_k(i)n \geq \epsilon n\right) \\ &= \Pr\left(\sum_{i=1}^L \alpha'_k(i) \leq L - \epsilon\right). \end{aligned} \quad (\text{A.3})$$

for any  $\epsilon > 0$ . Replacing (A.2) into this last expression yields:

$$\begin{aligned}
& \Pr(b_k(L) - b_k(0) \geq \epsilon n) \\
&= \Pr\left(\sum_{i=1}^L \frac{\log_2(1 + \text{SNR}\gamma_k(i))}{\bar{R} - \delta} \leq L - \epsilon\right) \\
&= \Pr\left(\sum_{i=1}^L \log_2(1 + \text{SNR}\gamma_k(i)) - L\bar{R} \leq (\epsilon - L)\delta - \epsilon\bar{R}\right) \\
&= \Pr\left(\sum_{i=1}^L \frac{\log_2(1 + \text{SNR}\gamma_k(i)) - \bar{R}}{\sqrt{L \text{Var}(R)}} \leq \frac{(\epsilon - L)\delta - \epsilon\bar{R}}{\sqrt{L \text{Var}(R)}}\right), \tag{A.4}
\end{aligned}$$

where we have defined

$$\text{Var}(R) \triangleq \mathbb{E}_\gamma \left[ \left( \log_2(1 + \text{SNR}\gamma(i)) - \bar{R} \right)^2 \right]. \tag{A.5}$$

For large  $L$ , we can resort to the central limit theorem by which

$$Z = \sum_{i=1}^L \frac{\log_2(1 + \text{SNR}\gamma_k(i)) - \bar{R}}{\sqrt{L \text{Var}(R)}} \sim \mathcal{N}(0, 1). \tag{A.6}$$

Hence, as long as  $\delta$  takes strictly positive values ( $\delta > 0$ ), we have that

$$\begin{aligned}
& \lim_{L \rightarrow \infty} \Pr(b_k(L) - b_k(0) \geq \epsilon n) \\
&= \lim_{L \rightarrow \infty} \Pr\left(Z \leq \frac{(\epsilon - L)\delta - \epsilon\bar{R}}{\sqrt{L \text{Var}(R)}}\right) = 0. \tag{A.7}
\end{aligned}$$

This result states that, as long as we encode a slightly higher number of samples per timeslot (which depends on parameter  $\delta$ ) the probability that the increase in buffer occupancy exceeds  $\epsilon n$  samples (for a *finite* value of  $\epsilon$ ) can be made arbitrary small for large  $L$ . That is, buffers are stable. Conversely,  $\delta = 0$  yields

$$\lim_{L \rightarrow \infty} \Pr(b_k(L) - b_k(0) \geq \epsilon n) \stackrel{\delta=0}{=} \frac{1}{2}, \tag{A.8}$$

this meaning that, even for arbitrarily large values of  $\epsilon$ , the probability that buffer occupancy increases beyond  $\epsilon n$  is unavoidably 1/2 (i.e., unstable buffers).

In addition to this main result, the probability for buffers to drain after  $L$  timeslots can be expressed as

$$\begin{aligned}
p_{\text{drain}} &= \Pr(b_k(L) = 0) \\
&= \Pr\left(\sum_{i=1}^L \alpha'_k(i)n \geq (L + L_0)n\right) \\
&= \Pr\left(\sum_{i=1}^L \frac{\log_2(1 + \text{SNR}\gamma_k(i))}{\bar{R} - \delta} \geq L + L_0\right). \tag{A.9}
\end{aligned}$$

By resorting again to the central limit theorem, we have that for any positive value of  $\delta$

$$\lim_{L \rightarrow \infty} p_{\text{drain}} = \lim_{L \rightarrow \infty} \Pr\left(Z \geq \frac{L_0\bar{R} - (L + L_0)\delta}{\sqrt{L \text{Var}(R)}}\right) = 1, \tag{A.10}$$

and, thus, buffers will drain with probability one after a sufficiently large number of timeslots.

## Acknowledgment

This work is partly supported by the Catalan Government (2009 SGR 1046), the EC-funded project NEWCOM++ (216715), and the Spanish Ministry of Science and Innovation (FPU grant AP2007-01654).

## References

- [1] I. F. Akyildiz, W. Su, Y. Sankarasubramaniam, and E. Cayirci, "Wireless sensor networks: a survey," *Computer Networks*, vol. 38, no. 4, pp. 393–422, 2002.
- [2] M. C. Vuran and I. F. Akyildiz, "Spatial correlation-based collaborative medium access control in wireless sensor networks," *IEEE/ACM Transactions on Networking*, vol. 14, no. 2, pp. 316–329, 2006.
- [3] S. C. Draper and G. W. Wornell, "Side information aware coding strategies for sensor networks," *IEEE Journal on Selected Areas in Communications*, vol. 22, no. 6, pp. 966–976, 2004.
- [4] A. D. Wyner and J. Ziv, "The rate-distortion function for source coding with side information at the decoder," *IEEE Transactions on Information Theory*, vol. 22, no. 1, pp. 1–10, 1976.
- [5] P. Ishwar, A. Kumar, and K. Ramchandran, "Distributed sampling for dense sensor networks: a bit-conservation principle," in *Proceedings of the 2nd International Workshop on Information Processing in Sensor Networks*, vol. 2634 of *Lecture Notes in Computer Science*, pp. 17–31, April 2003.
- [6] D. Dardari, A. Conti, C. Buratti, and R. Verdone, "Mathematical evaluation of environmental monitoring estimation error through energy-efficient wireless sensor networks," *IEEE Transactions on Mobile Computing*, vol. 6, no. 7, pp. 790–802, 2007.
- [7] A. Dogandžić and K. Qiu, "Decentralized random-field estimation for sensor networks using quantized spatially correlated data and fusion-center feedback," *IEEE Transactions on Signal Processing*, vol. 56, no. 12, pp. 6069–6085, 2008.
- [8] M. Dong, L. Tong, and B. M. Sadler, "Impact of data retrieval pattern on homogeneous signal field reconstruction in dense sensor networks," *IEEE Transactions on Signal Processing*, vol. 54, no. 11, pp. 4352–4364, 2006.
- [9] D. Marco and D. L. Neuhoff, "Reliability vs. efficiency in distributed source coding for field-gathering sensor networks," in *Proceedings of the 3rd International Symposium on Information Processing in Sensor Networks (IPSN '04)*, pp. 161–168, Berkeley, Calif, USA, April 2004.
- [10] I. Karatzas and S. E. Shreve, *Brownian Motion and Stochastic Calculus*, Springer, 1988.
- [11] S. Finch, "Ornstein-uhlenbeck process," May 2004, <http://algo.inria.fr/resolve/ou.pdf>.
- [12] S. M. Kay, *Fundamentals of Statistical Signal Processing: Estimation Theory*, Prentice-Hall Signal Processing Series, Prentice-Hall, Englewood Cliffs, NJ, USA, 1993.
- [13] T. M. Cover and J. A. Thomas, *Elements of Information Theory*, Wiley Series in Telecommunications, Wiley, New York, NY, USA, 1993.
- [14] P. Ishwar, R. Puri, K. Ramchandran, and S. S. Pradhan, "On rate-constrained distributed estimation in unreliable sensor networks," *IEEE Journal on Selected Areas in Communications*, vol. 23, no. 4, pp. 765–775, 2005.

- [15] R. M. Corless, G. H. Gonnet, D. E. G. Hare, D. J. Jeffrey, and D. E. Knuth, "On the Lambert  $W$  function," *Advances in Computational Mathematics*, vol. 5, no. 4, pp. 329–359, 1996.
- [16] C. D. Meyer, *Matrix Analysis and Applied Linear Algebra*, SIAM, 2001.
- [17] M. F. Neuts, *Matrix-Geometric Solutions in Stochastic Models: An Algorithmic Approach, Chapter 2: Probability Distributions of Phase Type*, Dover, 1981.